Increasing PV Hosting Capacity in Distorted Distribution Systems Using Passive Harmonic Filtering

Selcuk Sakar, [a]* Murat E. Balci[a], Shady H.E. Abdel Aleem[b], Ahmed F. Zobaa[c]

[a]Electrical and Electronics Engineering, Balikesir University, Balikesir, Turkey (email: sakar.selcuk@gmail.com)
[a]Electrical and Electronics Engineering, Balikesir University, Balikesir, Turkey (email: mbalci@balikesir.edu.tr)
[b]15th of May Higher Institute of Engineering, Mathematical and Physical Sciences, Helwan, Cairo, Egypt (email: engyshady@ieee.org)
[c]College of Engineering, Design & Physical Sciences, Brunel University London, Uxbridge United Kingdom (email: azobaa@ieee.org)
*Corresponding author: T: +905413767099 | E-mail address: sakar.selcuk@gmail.com

***Abstract*—**Adding new capacity expansion alternatives using distributed generation (DG) technologies, particularly penetration of renewable energy, has several economical, and technical advantages such as the reduced system costs, the improved voltage profile, lower line loss and enhanced system's reliability. However, the DG units may lead to power quality, energy efficiency, and protection problems in the system when their penetration exceeds a particular value, generally called as the system's hosting capacity (HC) in the literature. In this paper, the HC determination of a distorted distribution system with Photovoltaic (PV)-based DG units is handled as an optimization problem by considering over and under voltage limitations of buses, current carrying capabilities of the lines, and harmonic distortion limitations as constraints. It is seen from simulation results that the HC is dramatically decreased with the increament of the load's nonlinearity level and the utility side's background voltage distortion. Accordingly, a *C*-type passive filter is designed to maximize the harmonic-constrained HC of the studied system while satisfying the constraints. The results indicate that higher HC level can be achieved using the proposed filter design approach compared to three conventional filter design approaches as voltage total harmonic distortion minimization, line loss minimization and power factor maximization.

Keywords— Distributed generation; harmonic analysis; hosting capacity; optimization; passive filters; power quality; PV systems.

1. INTRODUCTION

Distributed generation (DG) technologies are small-scale dispersed sources of electric power, which are placed close to the loads being served [1]-[3]. Many DG technologies exist such as photovoltaic (PV) cells, wind turbines, biomass, small hydro, micro-turbines, fuel cells, and others. DG technologies have been widely practiced in the distribution systems since they provide technical benefits for the power networks such as voltage profile improvement, system reliability and security enhancement, power loss reduction, and energy efficiency increase. Furthermore, energy crisis caused by the shortage of the traditional energy resources such as natural gas and petroleum, and the expanded interests to global warming and climate change have forced all the stakeholders including planners of distribution companies to focus on the widely employement of the DG technologies using environmentally friendly renewable energy resources [4]. Socially, renewable energy–based industries are more labor-intensive compared to fossil fuel–based technologies because of their continued development process. Hence, the investment in the DG technologies may represent a real opportunity to meet the load growth by adopting low-cost, low-carbon, and high-efficient capacity expansion alternatives [5], [6].

In the past, the grid interconnected DG units were weaker to cause a significant disturbance in the distribution system. Currently, with the notable progress in systems integration with dispersed generation units, this situation is changing, and the dream of 100% penetration is getting closer. However, excessive penetration or inappropriate DG capacities may produce undesirable effects in the electrical systems such as power quality, energy efficiency, and protection problems [7], [8]. The possible amount of DG penetration that can safely be handled by grids is called as hosting capacity (HC). Hence, specifying the appropriate penetration of DG units without violating the hosting limit is a principal factor for increasing the benefits gained from them. Accordingly, optimal planning, placement, and sizing of DG units in the distribution networks are considered in many works [9], [10].

In the literature, different design goals are considered for the optimal planning problem of DG units such as the reduction of the system power losses [11], reactive power management [12], voltage profile enhancement [13], system security and reliability improvement [14], and maximizing of the DG penetration. Usually, the conventional design constraints are related to the voltage limitations represented by the voltage variation range and overvoltages, or current limitations posed by the allowable loading capabilities of the lines/cables and transformers, or DG limitations represented by their types, numbers, sizes, and economics. However, with the increase of power electronic-based loads (nonlinear loads) and using of large-scale grid-connected DG units; today’s power systems suffer from harmonic pollution represented by harmonic voltage and current distortions. Increased levels of harmonic pollution can cause excessive losses or heating of all kinds of equipment as supply lines, transformers, power factor correction capacitors and induction motors; reducing their lifetimes [15].

Besides, they can reduce the energy transfer efficiency or transmission power factor [16], [17]. To overcome these harmonics related problems, the international standards such as IEEE Standard 519 and IEC 61000-3-2 provide limits for individual and total harmonic distortion of PCC voltages and currents [18].

Many studies investigated the impact of the harmonic distortion generated by the DG units on the HC of distribution systems [19]-[26]. In [19], for radial distribution feeders with different load patterns, closed-form expressions were derived to determine the allowable penetration levels of DG units without exceeding the voltage harmonic distortion limits. In [20], an optimization problem was formulated for estimation of the allowable DG penetration level in the IEEE 18-bus benchmark system, while meeting a restricted voltage range and satisfying IEEE 519 limitations for total and individual voltage harmonic distortion. It was concluded in the same study that adding harmonic limitations in DG interconnection studies is important to restrict the harmonic distortion associated effects. In [21], it was figured out that power factor correction capacitors may lead to resonance hazards in a system with the PV-based DG units; consequently, harmonic filters should be used to increase the harmonic-constrained permissible PV capacities of the systems. Similarly, [22] pointed out that harmonic filters should be employed for the improvement of the maximum allowable DG penetration level. In [23], a DG planning problem based on maximizing the DG penetration level considering the bus voltage limits and the IEEE 519 allowable voltage harmonic limits was solved in the IEEE 18-bus test system for ten loads and DG scenarios. The most significant result obtained in the same study is that decentralization of DG capacity could be used to attain higher DG penetration levels. Furthermore, [24] introduced the harmonic-constrained hosting capacity term, which means the hosting capacity by considering voltage harmonic distortion limits. It proposed a methodology to determine this constrained capacity by regarding the Norton equivalent harmonic model of the system seen from the connection point of the DG unit. Also, it presented the best and the worst conditions of the harmonic hosting capacity when the harmonic currents, which are injected by the utility and the DG unit, are in the same and reverse directions, respectively. In [25], a multi-criteria optimization problem of the simultaneous planning of passive filters and DG units was solved to minimize bus voltage total harmonic distortions, total line loss and investment costs of the filters and DG units. Also, [26] solved the same placement problem for inverter-based DG units and capacitor banks regarding voltage support and loss reduction, and it concluded that harmonic distortion constraints should be included in the planning problems of the inverter-based DG units.

In this paper, the HC determination of a distorted distribution system containing Photovoltaic (PV)-based DG units is considered as an optimization problem by taking into account over and under voltage limitations of buses, current carrying capabilities of the supply lines, and harmonic distortion limitations such as maximum permissible total and individual harmonic distortion levels of the current

and voltage. Thus, in the first part of the paper, for the PV-based DG units, the hosting capacity of a typical two bus distribution system is parametrically analysed under various utility side's background voltage distortion and load's current distortion (or the load's nonlinearity level).

In the second part of this paper, optimal passive harmonic filter design approach is proposed to maximize the hosting capacity while satisfying the above mentioned constraints and the desired power factor level. The proposed approach can be implemented for any kind of filter. However, in this study, the proposed approach is demonstrated with the *C*-type filters since they do not have resonance problem and have low power loss at the fundamental frequency compared to other passive filter types [27]-[29].

Finally, to show the effectiveness of the proposed filter design approach, the results of the proposed one and three conventional filter design approaches, which are based on voltage total harmonic distortion minimization, line loss minimization and power factor maximization, are comparatively evaluated for the studied system.

2. METHODS

In this section, background on the HC control, problem formulations of the proposed and conventional filter designs approaches, and the search algorithm developed for simultaneous sizing of DG unit and the passive filter will be presented:

2.1. Hosting capacity control

Generally, the term "penetration" concerns with the peak load or energy on a yearly time-scale. In this work, the peak instantaneous penetration (PIP) is regarded as the ratio of the DG power to the load's rated power. For a particular system, the PIP ratio is a proper measure for studying the impact of the DG's power on the power quality of the system [30]. In this regards, the HC of distribution networks indicates the DG penetration level that the grid can withstand before violating anyone of the performance indices [31], as illustrated in Fig. 1.

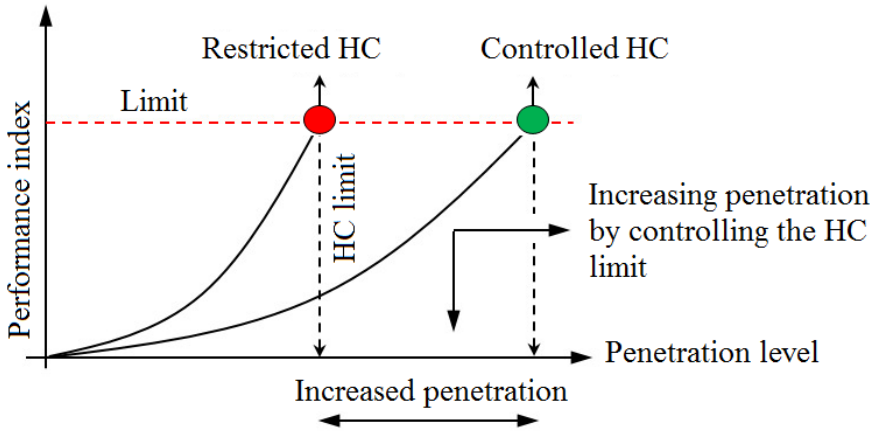

Fig. 1 Conception of the HC

It is seen from this figure that the increament of the DG penetration is limited by performance indices. Under sinusoidal conditions, the first and the most important performance index is the bus voltage, as overvoltage will occur with introducing a DG unit into a particular bus; hence, it should be limited. The second main index is the current carrying capability of the lines/cables, and the third index that may be taken into consideration is the substation transformer's power [32]. However, under non-sinusoidal conditions, the maximum permissible values of the total and individual harmonic distortion indices provided by the international standards limits the DG penetration level or the system's HC; hence, suitable corrective actions should be employed to mitigate them. For example, for the simplified 2-bus distribution system given in Fig. 2, the voltage rise (ΔV) due to a DG unit connection can be expressed as follows:

$$\Delta V = V_L - V_S \cong \frac{P*R}{|V_S|} + \frac{Q*X}{|V_S|} \quad (1)$$

V_S is the nominal system voltage, *i.e.* the voltage at the slack bus, and V_L is the voltage at the load bus. R and X are the equivalent resistance and reactance of the line/cable and transformer, respectively. P and Q are the net active and reactive power injected into the system, respectively.

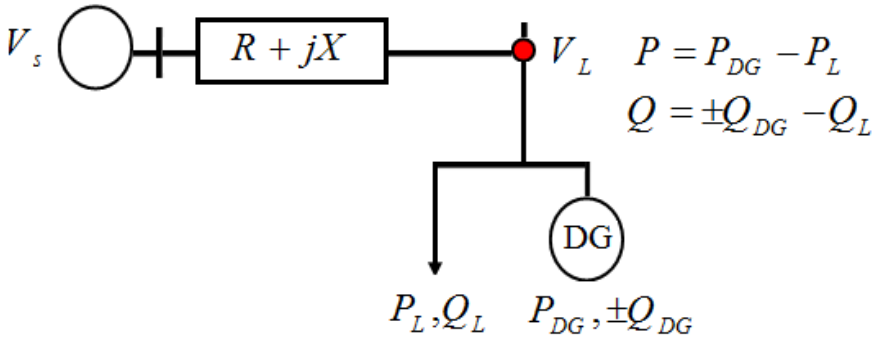

Fig. 2 Simplified 2-bus system with a DG unit connected at the load bus

It is clearly seen from (1) that the factors affecting the voltage rise (ΔV) and hence the HC are the $|V_S|$, (P*R), and (Q*X). Firstly, $|V_S|$ is a parameter specified by the distribution system operator, and it can be controlled by adjusting the set-point of the on-load tap changers in the substation transformers or replacing cables with thicker ones. The cable reinforcement (or replacing cables with thicker ones) will decrease the cable's impedance parameters as R and X, the voltage drop across it, and increase its current carrying capability. However, this solution is not always possible because of the economic considerations. Also, reactive power management can successively be implemented to control Q either by controlling the power factor of the inverter or by supporting the reactive power using capacitor banks. In the case of distorted systems, harmonic filters should be replaced with the capacitor banks. Moreover, an active power control can be planned using energy storage techniques or reactive power

curtailment. Here, it should be noted that choosing the right solution may depend on other factors such as (Q/P) or (X/R) ratios.

One can see from the explanations given up to now that the HC index can be controlled and increased to allow its higher values. Accordingly, in this work, two main goals are desired:

(i) Evaluation of the HC of distorted distribution systems, and showing the effect of the harmonic distortion on the system's HC, while considering background voltage distortion, DG harmonic currents, and various nonlinearity levels of the loads.

(ii) Increasing of the harmonic-constrained HC by using passive filtering, while satisfying the common requirements implied in the DG optimization problems.

2.2. Problem formulation

Detailed modeling of the system under study and the problem formulations of the proposed and traditional optimal filter design approaches are given as follows:

2.2.1. The system under study

Single line diagram of the studied typical two bus distribution system is given in Fig. 3. It consists of a symmetric distribution line, a group of balanced linear and nonlinear loads, PV-based DG units with their transformer, and a passive harmonic filter. This system except DG units was considered as a benchmark system to test the performance of optimal passive filter designs in many works [27]-[29]. In the considered benchmark system, the nonlinear load is the six-pulse rectifier, which is one of the most widely used non-linear loads.

For straight forward and accurate frequency domain analysis, the load side of the studied system is modelled as a combination of harmonic current sources and passive circuit elements. In addition, its utility side is represented using its *h*th harmonic Thevenin equivalent circuit. By taking into consideration the harmonic model of the system, the harmonic power flow (HPF) method is used to calculate the currents/voltages of the system for each harmonic order *h*. The HPF has three sequential steps as follows:

(i) Running power flow analysis for the fundamental frequency. In this study, the Newton-Raphson (NR) algorithm, which is well-known in the literature, is used for power flow analysis [25]. For the power flow at the fundamental frequency; utility and load buses are modelled as slack and PQ buses, respectively, and the admittance matrix represents the distribution line.

(ii) Updating the harmonic impedances of the linear loads and the harmonic currents of the nonlinear loads and the PV-based DG units according to the results of the fundamental power flow.

(iii) Calculation of the non-fundamental harmonic bus voltages using the nodal equations at each harmonic order, as follows:

$$[Y^h][V^h] = [I^h] \tag{2}$$

The *h*th harmonic load admittance (y_{load}^h), and line admittance (y_{line}^h) are expressed respectively, as follows [34]:

$$y_{load}^h = \frac{1}{Z_{load}^h} = \frac{P_L^1}{|V_L^1|^2} - j\frac{Q_L^1}{h|V_L^1|^2} \tag{3}$$

$$y_{line}^h = \frac{1}{Z_{line}^h} = \frac{1}{R_{line}^h + jX_{line}^h} \tag{4}$$

where $|V_L^1|$, P_L^1, and Q_L^1 represent the PCC rms voltage (phase-to-neutral), single-phase active power of the linear load, and single-phase reactive power of the linear load, respectively, at the fundamental frequency. R_{line}^h and X_{line}^h represent the *h*th harmonic supply line's resistance, and supply line's reactance, respectively. Also, Z_{load}^h and Z_{line}^h are the *h*th harmonic impedance of the load and the line, respectively.

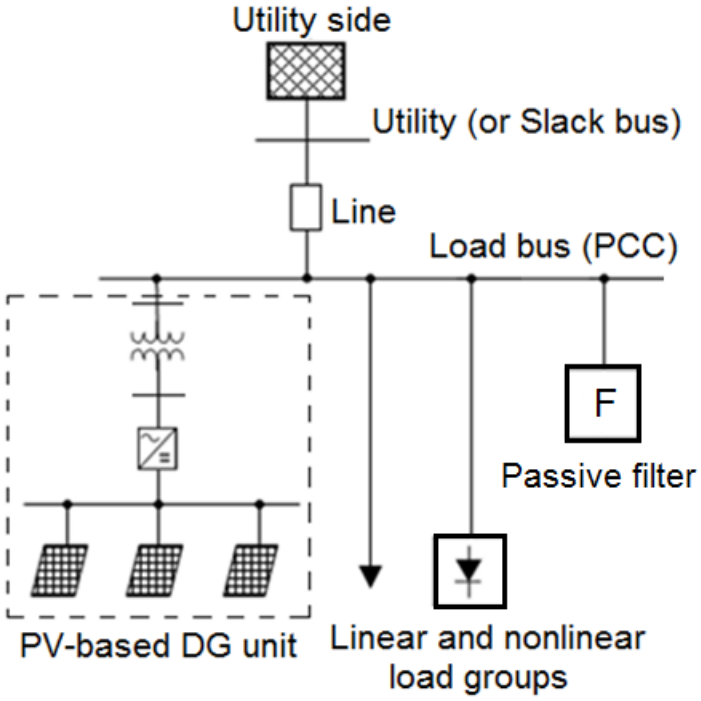

Fig. 3 The system under study

Linear load group are modelled as a parallel combination of a resistance in parallel with a reactance [25]. Nonlinear loads are modelled as a current source I_C^h that injects harmonic current into the system at harmonic order *h*, and this can be formulated as follows:

$$I_C^h = C(h)I_C^1 \tag{5}$$

so that,

$$I_C^1 = \left[\frac{(P_{NL}^1 + jQ_{NL}^1)}{V_L^1}\right]^* \tag{6}$$

where, P_{NL}^1 and $Q_{NL}^1$are the nonlinear loads' active power and reactive power at the fundamental, respectively.

In this work, according to the harmonic domain model of DG units widely considered in the literature [21]- [23], the harmonic current emission of the PV-based DG units (I_{DG}^{h}) is assumed to change linearly with their total installed power of the DG (P_{DG}), so that;

$$I_{DG}^{h} = I_{spectrum}^{h} \frac{P_{DG}}{V_{bus}} \tag{7}$$

where $I_{spectrum}^{h}$ represents the harmonic spectrum of a typical PV-based DG unit [26]. This model is based on the rated power of the PV inverters. Depending on the phase angles of the harmonic currents generated by the nonlinear loads and the PV-based DG units, the resultant phasor nonlinear current ($\overline{I^{h}}$) can be given as follows:

$$I_h = I_C^h - I_{DG}^h \tag{8}$$

Different nonlinear types of equipment connected to a PCC indeed have different harmonic spectra. However, the resultant current from their combination is in general lower than the arithmetic sum of their magnitudes [24]. Let us assume two distorted currents with different harmonic spectra; the resulting current from their phasor combination will have the lowest distortion when the phase difference is 180 degrees (π radians) between the two harmonic sources. Hence, we can say that the best phasor scenario will take place when the currents are in anti-phase. On the contrary, the resulting current from their phasor combination will have the highest distortion when the phase difference equals zero. Hence, we can say that the worst phasor scenario (arithmetic sum) will take place when the currents are in-phase.

On the other hand, according to IEC standard 61000-3-6 [33], the sum of the harmonic currents drawn by the nonlinear load and DG units can be found in the case of unknown phase angles as follows:

$$I_{h,sum}^{\sigma} = \sum_i I_{h,i}^{\sigma} \tag{9}$$

where σ is the summation exponent, $I_{h,sum}^{\sigma}$ is the resultant harmonic current from summation, and $I_{h,i}^{\sigma}$ is the *i*th individual harmonic components of the same order. Also, σ varies according to the harmonic order, as follows [33]:

$$\sigma = \begin{cases} 1, & if\ \ h < 5 \\ 1.4, & if\ \ 5 \le h \le 15 \\ 2, & if\ \ h > 15 \end{cases} \tag{10}$$

Besides, a linear summation is assumed for the identical inverters of the PV-based DG units, *i.e.* harmonic content increases with the penetration of DG. In the case of multiple different inverters in grid-connected large-size PV installations, another formula using harmonic summation ratio (ζ_h) may be employed with different weighting factors. Readers could refer to [34] for more details about equal ($\zeta_h = 0$), linear ($\zeta_h = 1$), and Euclidean ($\zeta_h = \frac{1}{\sqrt{N}}$) summations under such cases, where *N* is the number of inverters.

In Fig. 3, *F* denotes a *C*-type passive filter. Fig. 4 shows the single-phase equivalent circuit of the *C*-type filter. In general, it is a high-pass filter that provides sufficient harmonic filtering for a broad range of harmonics, damps resonance may occur, and has very low power loss compared to other passive filter types [27]- [29].

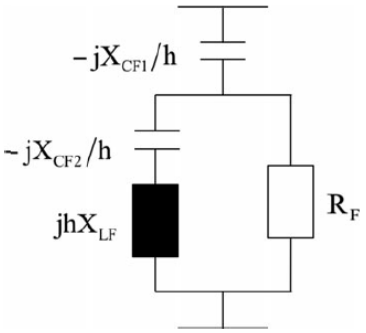

Fig. 4 Single-phase equivalent circuit of the *C*-type filter

It consists of the main capacitive reactance (X_{CF1}) in series with a parallel combination of series branch, of inductive reactance (X_{LF}) - capacitive reactance (X_{CF2}), and a damping resistor (R_F). X_{CF1} provides the required capacitive compensation at the fundamental frequency to compensate the reactive power which is necessary for supporting voltage and reducing line loss and improving the power factor (*PF*). The inductive reactance (X_{LF}) and the capacitive reactance (X_{CF2}) should be equal at the fundamental frequency, *i.e.* (X_{CF2}=$X_{LF} = X_F$), to bypass the resistor for the fundamental harmonic. The *h*th harmonic impedance can be expressed as;

$$Z_{filter}^{h} = -j\frac{X_{CF1}}{h} + \frac{jR_F X_F(h^2-1)}{hR_F + jX_F(h^2-1)} \tag{11}$$

Therefore, for the equivalent circuit of the studied system given in Fig. 3, the harmonic phase voltage V_L^h at the point of common coupling (PCC) between the utility system and the consumer can be calculated using Equation (12) as follows:

$$V_L^h = \left[\frac{V_S^h}{Z_{line}^h} - I^h\right]\left[\frac{1}{Z_{line}^h} + \frac{1}{Z_{load}^h} + \frac{1}{Z_{filter}^h}\right]^{-1} \tag{12}$$

Also, the *h*th harmonic line current I_{line}^h is expressed as follows:

$$I_{line}^h = \frac{V_S^h - V_L^h}{Z_{line}^h} \tag{13}$$

where, V_S^h represents the *h*th harmonic substation voltage. Finally, the active line losses (ΔP_{line}), and the filter loss (ΔP_{filter}) can be expressed, respectively, as follows:

$$\Delta P_{loss} = \sum_{h=1}^{h_{max}} \left|I_{line}^h\right|^2 Re\{Z_{line}^h\} \tag{14}$$

$$\Delta P_{filter} = \sum_{h=1}^{h_{max}} \left|\frac{V_L^h}{Z_{filter}^h}\right|^2 Re\{Z_{filter}^h\} \tag{15}$$

2.2.2. The proposed filter design

The objective of the simultaneous sizing of the passive filter and the PV-based DG units is to achieve the maximum allowable penetration which can safely be hosted by the distorted distribution network. Equations (16) and (17) mathematically define the HC and the proposed objective function (OF_1), respectively.

$$HC\ (\%) = \frac{P_{DG}}{S_{rated}} * 100 \tag{16}$$

$$OF_1 = Maximize\ HC = f_1(X_{CF1}, X_F, R_F, P_{DG}) \tag{17}$$

where P_{DG} represents the capacity of the PV-based DG units, and S_{rated} represents the rated power of the DG/load bus. Various constraints are formulated to guarantee the DG penetration level without violating the performance indices:

(i) Bus voltage limits: The bus rms voltage (V_L^{rms}) should be confined within its predetermined minimum and maximum limits, denoted as $V_{L,min}^{rms}$ and $V_{L,max}^{rms}$, respectively, so that:

$$V_{L,min}^{rms} \leq \sqrt{|V_L^1|^2 + \sum_{h=2}^{hmax} \left|V_L^h\right|^2} \leq V_{L,max}^{rms} \tag{18}$$

According to the ANSI C84.1 guidelines [35], $V_{L,min}^{rms}$ and $V_{L,max}^{rms}$ are considered as 0.95 p.u. and 1.05 p.u, respectively.

(ii) Total harmonic distortion limits: The IEEE Std. 519-2014 imposes limits on the voltage total harmonic distortion (THDV) at the PCC, as follows:

$$THDV\ (\%) = \frac{\sqrt{\sum_{h>1} |V_L^h|^2}}{|V_L^1|} * 100 \leq THDV_{max}(\%) \tag{19}$$

Also, the total demand distortion (TDD) measured at the PCC should be limited, so that;

$$TDD(\%) = \frac{\sqrt{\sum_{h>1} |I_{line}^h|^2}}{\mathrm{I}_R} 100 \leq TDD_{max}(\%) \tag{20}$$

where, $THDV_{max}$ and TDD_{max} signify the maximum values permitted by IEEE 519 for both the *THDV* and *TDD*, respectively. Also, I_R is the rated line current.

(iii) Individual harmonic distortion (IHD) limits: The IEEE Std. 519 demands users to limit the individual harmonic voltages V_L^h and currents I_{line}^h measured at the PCC so that the weekly 95th percentile short-time (10 minutes) harmonic voltages/currents should be less than specific values that depend on voltage level, frequency range, and system strength. The *h*th harmonic individual voltage and current harmonics, denoted as $IHDV_h$ and $IHDC_h$, should be limited as follows:

$$IHDV_h\ (\%) = \left|\frac{V_L^h}{V_L^1}\right| * 100 \leq IHDV_{max}(\%) \tag{21}$$

$$IHDC_h\ (\%) = \left|\frac{I_{line}^h}{I_{line}^1}\right| * 100 \leq IHDC_{max}(\%) \tag{22}$$

where $IHDV_{max}$ and $IHDC_{max}$ represent their maximum allowed values documented in IEEE 519.

(iv) Current carrying capability of the supply line: Regarding distorted line/cable currents; harmonic derating factor (HDF) or the current carrying capability of the line/cable [29] should not exceed 100%, so that;

$$HDF\ (\%) = \sum_{h\geq 2}\left(\frac{R_{line}^{h}}{R_{line}^{1}}\right)\left|\frac{I_{line}^{h}}{I_{line}^{1}}\right|^{2} * 100 \leq 100(\%) \quad (23)$$

(v) DG capacity limit: To ensure the introduction of DG units into the distribution system will reduce all the net transmission power losses, the power provided by the DG units should not exceed a certain percentage of the total feeder load [26]. In this work, 100% penetration is taken as the limiting value. Additionaly, regarding the IEEE Std. 1547 for the interconnection of DG units with power networks [36], the DG units shall not change the bus voltage so it is assumed that the PV-based DG unit generates only active power, *i.e.* operating at unity power factor.

(vi) Power factor (PF) range: To increase the energy transfer efficiency of the system; the *PF* measured at the PCC should be maintained in its acceptable range, so that;

$$PF = \frac{P}{S} = \frac{3\sum_h |V_L^h|\left|I_{line}^h\right|\cos\theta_h}{3\sqrt{\sum_h |V_L^h|^2}\sqrt{\sum_h |I_{line}^h|^2}} \quad (24)$$

$$0.95 \leq PF \leq 1.00 \quad (25)$$

where *P* and *S* represent the true active and apparent power demand from the utility, respectively. Consecutively, the inequalities shown in (18) to (23), and (25) are formulated as nonlinear constraints in the optimization problem. All are represented as functions of the design variables X_{CF1}, X_F, R_F, and P_{DG}.

2.2.3. The traditional filter designs

In the analysis, three traditional objective functions for passive filter designs such as the *THDV* minimization, *TDD* minimization, and *PF* maximization, will comparatively be evaluated with the proposed optimal design approach. Their objective functions can be expressed as follows:

$$OF_2 = Minimize\ THDV = f_2(X_{CF1}, X_F, R_F) \quad (26)$$

$$OF_3 = Minimize\ \Delta P_{loss} = f_3(X_{CF1}, X_F, R_F) \quad (27)$$

$$OF_4 = Maximize\ PF = f_4(X_{CF1}, X_F, R_F) \quad (28)$$

All the traditional approaches subject to the same constraints presented for the proposed optimal design approach.

2.3. Search algorithm

The genetic algorithm (GA) is used to solve the presented search problems. GA method is a heuristic method, which is applied extensively in power engineering problems. Besides, GA was successfully used to solve the optimal passive filter design problem in the literature [37]. Briefly, the algorithm is initiated with a set of random solutions called population. Individuals from one population are evaluated based on the values of the OFs, *i.e.*, their fitness. The fitness is a figure of merit of the

individual or how well it fits with the required goals; the more fitness, the more likelihood of being chosen.

A selection procedure is performed for improving the population's fitness and keeping only the best individuals. Consequently, combining aspects of the selected individuals is undertaken to inherit their best features using the crossover. Small changes at random are involved to append randomness for the populations, which are represented by a mutation probability. Then, the algorithm will iterate to give the next generations until a termination condition is reached. Hence, the best solution is returned to designate the optimum (global) solution.

Regarding the minimization problems under study, the fitness functions are taken as the negative of the corresponding objective functions. For the maximization problem under study, the fitness function is considered the same as the objective function. Besides, the parameters of GA are set to a population size of 100 individuals, mutation probability equals 0.01, crossover probability equals 0.8, and a termination condition is set as 30 generations [38].

Fig. 5 shows a detailed flowchart of the proposed search algorithm to find the optimal size of the *C*-type filter and the HC of the considered system.

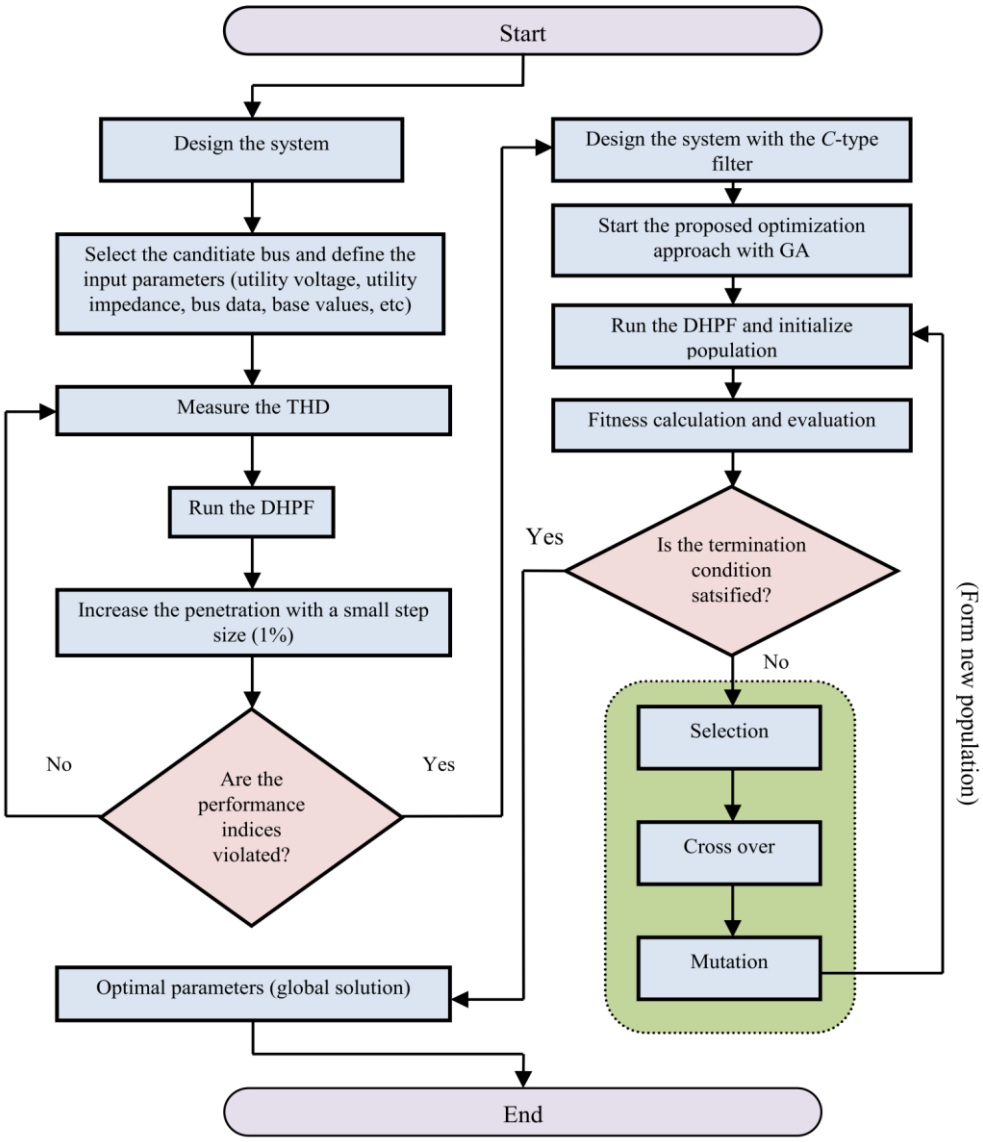

Fig. 5. The proposed search algorithm

3. RESULTS AND DISCUSSION

In this section, firstly, the DG hosting capacity of the studied system is parametrically analysed under various utility side's background voltage distortion and the load's nonlinearity level. Secondly, the results of the proposed and traditional optimal filter design approaches obtained by GA are comparatively evaluated to show the effectiveness of the proposed one on the hosting capacity improvement for the system under study. Thirdly, to point out the validity of the results provided by GA, the considered filter design problems are also solved by Grid Search (GS) method [29], which one of the well-known and the most reliable optimization methods.

3.1. Numerical data and design considerations

The studied system has 13.8 kV balanced three-phase source voltage at the fundamental frequency. It has a symmetric three-phase distribution line with voltage and current ratings as 13.8 kV and 314 amperes for an aluminium conductor with a cross-section area of 4/0 AWG and a length of

2.85 km. For fundamental harmonic, the resistance and inductive reactance values (R_{line}^{1} and X_{line}^{1}) of the distribution line are 0.855 Ω, and 1.165 Ω, respectively. The nonlinear loads are 6-pulse drive loads which have the harmonic current spectrum presented in Table 1 [39]. Besides, the harmonic spectrum of a typical PV-based DG unit is considered as shown in Table 2 [40]. To see the worst case of the HC under harmonically contaminated system conditions, the harmonic currents generated by the nonlinear loads and DG units are selected in-phase. Additionally, Table 3 [18] gives the IEEE Std. 519 limitations of the characteristic harmonic components of the studied system. According to the same standard, for the system, the limits of the total voltage harmonic distortion and total ($THDV_{max}$) demand distortion (TDD_{max}) are 5% and 8%, respectively.

Table 1
Harmonic current spectrum of typical 6-pulse nonlinear loads

h	5	7	11	13	17	19	23	25	29
Magnitude (%)	20	14.3	9.1	7.7	5.9	5.3	4.3	4.0	3.4

Table 2
Harmonic current spectrum of the PV-based DG unit [39]

h	Magnitude (%)	*h*	Magnitude (%)	*h*	Magnitude (%)
2	1.1294	12	0.7963	22	0.3980
3	3.2708	13	0.4559	23	0.2093
4	0.2624	14	1.0623	24	0.3538
5	3.4828	15	0.3045	25	1.3338
6	0.1244	16	0.5026	26	0.1925
7	1.1229	17	1.4810	27	0.6109
8	0.8193	18	0.5871	28	1.1996
9	0.4866	19	1.1377	29	0.8976
10	0.8423	20	0.7120	30	0.6741
11	0.6719	21	0.4987	31	0.4321

Table 3
IEEE Std. 519 limitations of the characteristic harmonic components of the system under study

h	5	7	11	13	17	19	23	25	29
$IHDV_{max}$ (%)					3.0				
$IHDC_{max}$ (%)	7.0	7.0	3.5	3.5	2.5	2.5	1.0	1.0	1.0

To properly evaluate the impact of the harmonic pollution on the system's HC and the filter performances, the system is simulated under various load-side's nonlinearity levels and utility-side's background voltage distortion:

(i) Load-side's nonlinearity level (NLL): The ratio of the apparent powers drawn by the nonlinear loads and total loads connected to the PCC increases gradually from 0% to 25%.

(ii) Utility-side 's background voltage distortion (BVD): The utility-side's background voltage distortion increases gradually from 0% to 4.5%. Table 4 presents the spectrum of BVD at 4.5%.

Table 4
Harmonic voltage spectrum of utility side's background voltage distortion

h	5	7	11	13	17	19	23	25	29
Magnitude (%)	3.0	2.0	2.0	1.0	1.0	1.0	1.0	0.5	0.5

Additionally, it is also aimed to investigate that the effect of the harmonic emission summation of the nonlinear load and DG on the analysis results. For this aim, two expressions are considered in the analysis. The first expression is the phasor or arithmetic sum given in (8), and the second one is the summation formula of the IEC 61000-3-6 standard [33] given in (9) and (10). In the phasor summation method, it is assumed that the harmonic angle is zero that it represents the worst harmonic aggregation between DG and nonlinear load.

3.2. Initial HC assessment

For the above mentioned NLL and BVD intervals, the HC value of the studied system without the filter is analysed here. As mentioned before, to find the HC value of the system, the penetration level of the PV-based DG units is increased from 0% with small steps. Thus, the maximum penetration level without the violation of the constraints given in (18)-(23) is determined as the HC. It should be noted that during the simulations, the substation voltage is assumed fixed at 13.8 kV, and the apparent power of the total load is kept at its rated value as 7.5 MVA. Therefore, for the considered NLL and BVD values, the contour of the HC are found by considering the IEC and the phasor summation rules. The results are given in Fig. 6. It is seen from Fig. 6 (a) that the HC based on IEC summation rule is found around 100% for the NLL values below 15%. Additionally, for the NLL values higher than %15, it considerably decreases under all BVD interval, and it is nil for the NLL and BVD values as 25% and 4.5%, respectively. On the other hand, Fig. 6 (b) shows that the HC based on phasor summation rule is strongly deteriorated with the increament of NLL and BVD. It has the highest value around 90% for both NLL and BVD values close to 0%, and it is nil for the NLL and BVD values as 25% and 4.5%.

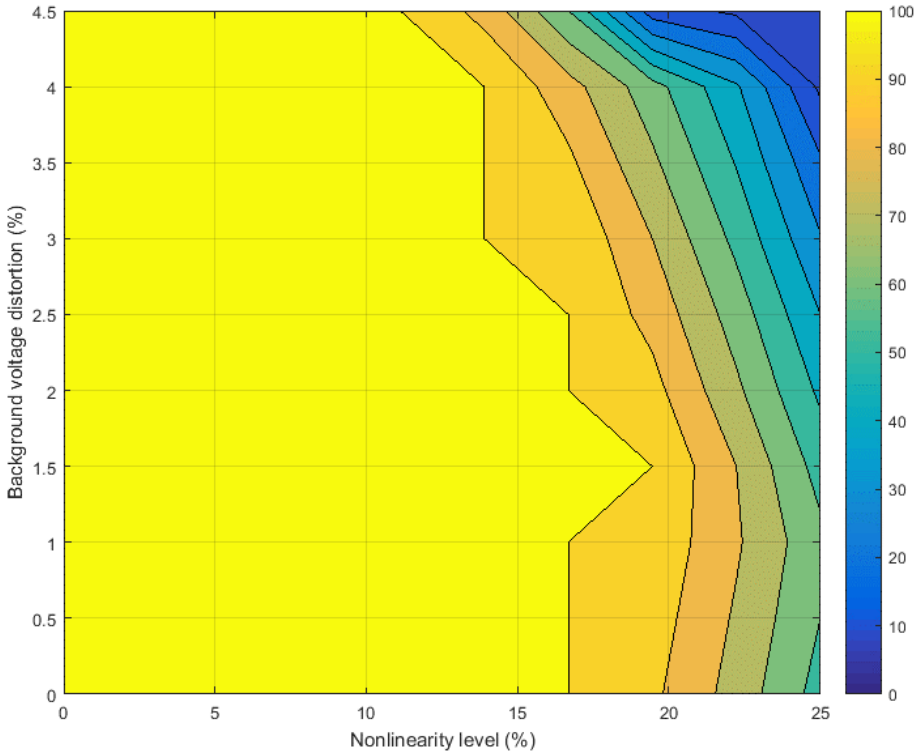

(a) Harmonic summation on the basis of the IEC summation rule

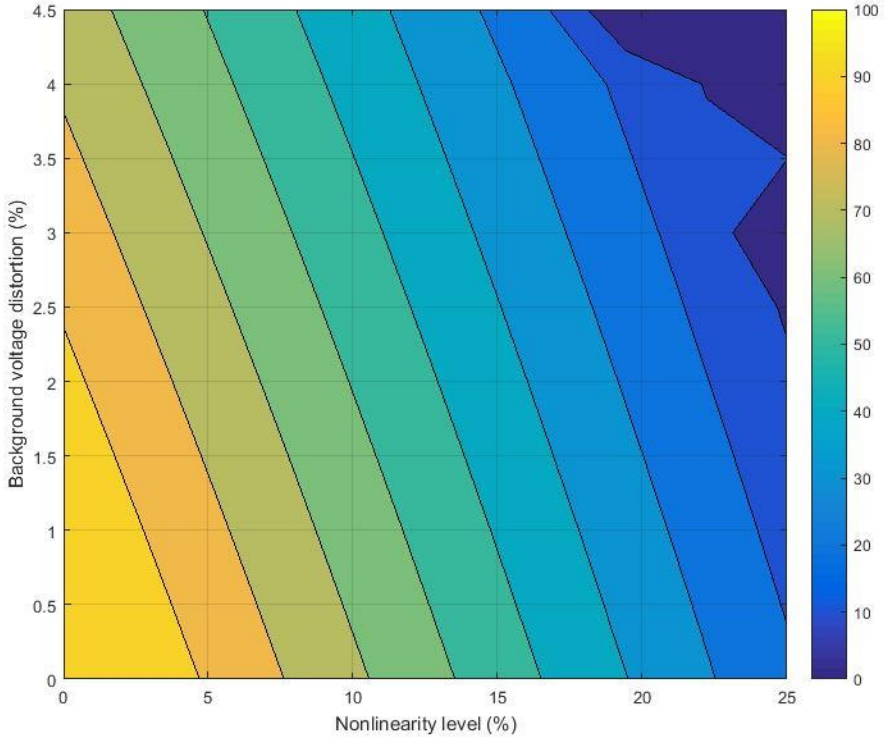

(b) Harmonic phasor summation

Fig. 6. Trends of the HC under non-sinusoidal conditions

In Fig. 7, for the DG penetration values between 0% and 100%, the variations of the most problematic performance indices as THDV, TDD, IHD_{23} and IHD_{25} are plotted under three NLL and BVD cases: nonsinusoidal utility voltage with moderate nonlinear load case (NLL=15% and BVD=4.5%), sinusoidal utility voltage with highly nonlinear load case (NLL=25% and BVD=0%) and nonsinusoidal utility voltage with highly nonlinear load case (NLL=25% and BVD=4.5%). Note that in this figure the performance indices have normalized values, and 1% is the normalized limit value for all of them. It is seen from Fig. 7 that the HC based on IEC summation rule is restricted by THDV and TDD in the nonsinusoidal utility voltage with moderate nonlinear load and sinusoidal utility voltage with highly nonlinear load cases, respectively. On the other hand, THDV and $IHDC_{25}$ are main factors to restrict the HC based on the phasor summation rule in both cases, respectively. Lastly, under the nonsinusoidal utility voltage with highly nonlinear load case, the HC based on IEC and phasor summation rules strongly depend on THDV and $IHDC_{25}$. It is also evident that including the harmonic limitations in the typical problem of maximizing the penetration considerably reduce the design freedom to host more capacity.

3.3. Increasing the HC using the proposed filter design

Impacts of the optimal filter designs on the HC are investigated for the system under study. For comparison among the filters designed according to the four OFs; the NLL and BVD are set at 25% and 4.5%, respectively. This perspective represents the highest right corner of Fig. 6 (worst point) under the most severe condition, *i.e.* zero percent penetration is possible, as validated in Fig. 6 and Figs 7(e) and 7(f). For this case, Table 5 gives the optimal parameters of the four different filter designs found by using both GA and GS optimization techniques. It is seen from the same table that all obtained filter designs have different R_F and X_F values. In addition, the size of the filters at fundamental frequency, which is represented by the reactive power ($Q_F = V_L^1 / X_{CF1}$), is slightly larger for the proposed one when compared to traditional three filter designs since X_{CF1} of the proposed filter design is slighltly lower than X_{CF1} values of the others. This may lead to a slight increament in the cost of the proposed one compared to the costs of the others.

For GA and GS methods, Table 6 presents values of the HC and performance parameters achieved by four optimal filter designs. Compared to the uncompensated system results included in Table 6, the designed filters increase the HC level, while enhancing the voltage, improving the power factor, and filtering the harmonics. However, the results can be considered comparable with regards to the performance indices, but this is not the case for the results of the HC. Moreover, straightforward objectives to minimize harmonic distortion (OF_2), or to maximize the power factor (OF_4) introduce low percentage of voltage and current distortions, respectively, but with considerably low hosting capacities.

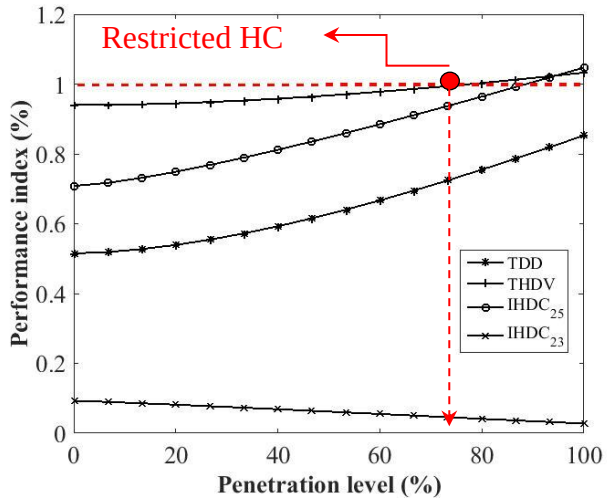

(a) 15% NLL and 4.5% BVD on the basis of the IEC summation rule

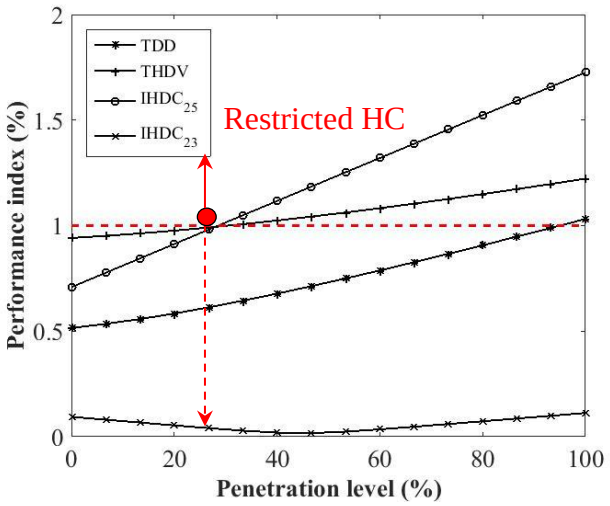

(b) 15% NLL and 4.5% BVD on the basis of the phasor summation

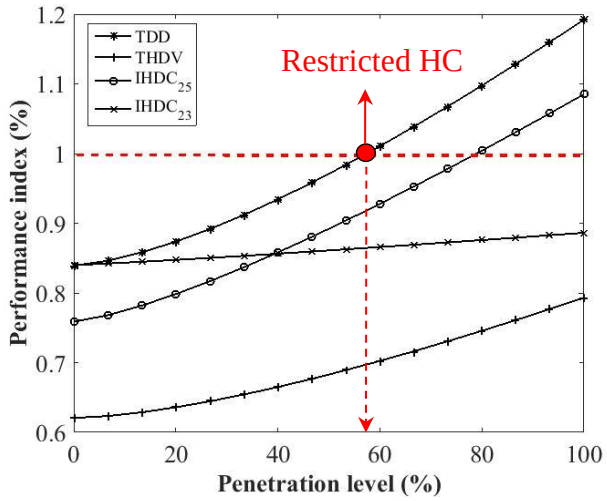

(c) 25% NLL and 0% BVD on the basis of the IEC summation rule

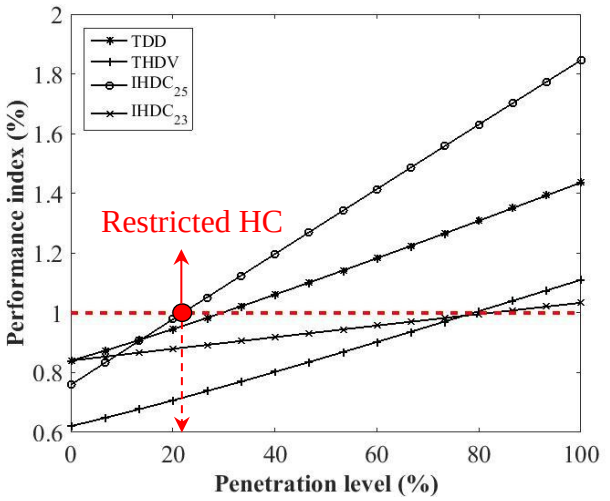

(d) 25% NLL and 0% BVD on the basis of the phasor summation

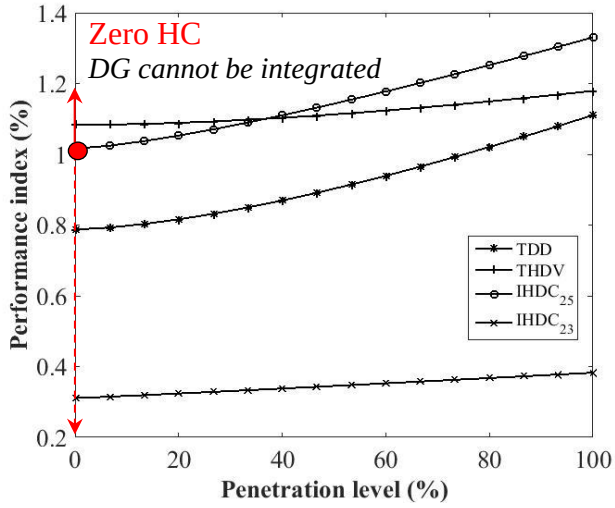

(e) 25% NLL and 4.5% BVD on the basis of the IEC summation rule

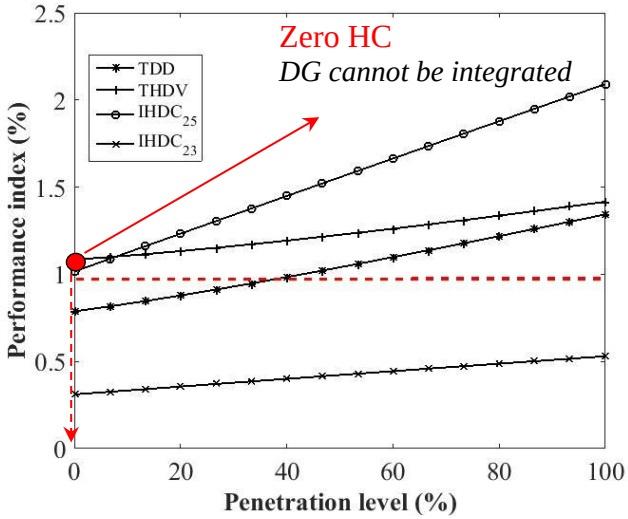

(f) 25% NLL and 4.5% BVD on the basis of the phasor summation

Fig. 7. Initial HC assessment at three distortion levels

Table 5
Optimal size of parameters of the designed filters

Objective functions	Algorithms					
	GA			GS		
	X_{CF1}(p.u.)	X_F(p.u.)	R_F(p.u.)	X_{CF1}(p.u.)	X_F(p.u.)	R_F(p.u.)
OF_1 (Max HC)	1.6808	0.1782	0.6374	1.6832	0.1769	0.6396
OF_2 (Min THDV)	1.7070	0.1175	1.0507	1.6856	0.1154	1.2332
OF_3 (Min ΔP_{loss})	1.6845	0.3569	3.0420	1.6844	0.3760	3.1231
OF_4 (Max PF)	1.6845	0.2451	0.9054	1.6856	0.2337	0.8874

Table 6
Performance indices and hosting capacities obtained using the designed filters

Parameters	No filter	Algorithms							
		GA				GS			
		OF_1	OF_2	OF_3	OF_4	OF_1	OF_2	OF_3	OF_4
THDV (%)	5.68	3.69	3.17	4.52	3.94	3.68	3.17	4.55	3.91
TDD (%)	7.10	7.79	7.99	6.04	6.75	7.79	7.99	6.04	6.80
PF (%)	77.43	99.75	99.68	99.69	99.78	99.75	99.65	99.69	99.78
ΔP_{loss} *(kW)*	224.25	184.87	184.95	184.28	184.50	184.87	185.02	184.27	184.57
HDF (%)	99.28	99.17	99.17	99.47	99.35	99.17	99.17	99.47	99.34
HC (%)	0.00	54.12	18.95	14.63	35.67	53.03	18.56	14.04	35.55

In addition to the above mentioned evaluations, it can be concluded from Table 5 and 6 that GA and GS optimization techniques give very close results for the considered optimization problem. As well as the capability to reduce the transmission losses, while satisfying the different design constraints, the filter design based on the proposed objective function (OF_1) results in considerably higher *HC* percentages compared to the considered three traditional filter designs. On the other hand, the designed filter based on OF_3 introduces the lowest HC value for the simulated case.

The effect on HC level of the proposed filter design, presented in Table 5 for NLL and BVD values as 25% and 4.5%, is investigated under the non-sinusoidal test conditions considered in Fig. 6. The results are plotted in Fig. 8. For all test conditions, 100% penetration of the DG unit is achieved with the proposed filter design if the HC is computed by regarding the IEC harmonic emission summation formula (see Fig. 8 (a)). However, this case is not observed for the HC computation based on phasor summation rule (see Fig. 8 (b)). Beside, it is seen from Fig. 6 (b) and 8 (b) that the proposed filter design improves the system's HC under all test cases except the small part around NLL=0% and BVD=4%. This means that it is capable of increasing the harmonic-constrained capacities under different harmonic distortion levels which validate the proposed filter robustness. In addition to these results, under the three particular cases of NLL and BVD aforementioned in Fig. 7, Fig. 9 shows the variation of the most problematic harmonic distortion indices with the increament of DG penetration level before and after adding the proposed filter design into the system. Fig. 9 (a) points out that the

harmonic distortion indices does not limit the HC based on the IEC summation rule for the system with the filter. However, it is seen from Fig. 9 (b) that this is not the case for the HC based on the phasor summation rule. In addition, the harmonic index, which limits the HC based on the phasor summation, can be different for the system without and with the proposed filter design. This means that for the maximization of the HC the filter design is not a straight forward problem.

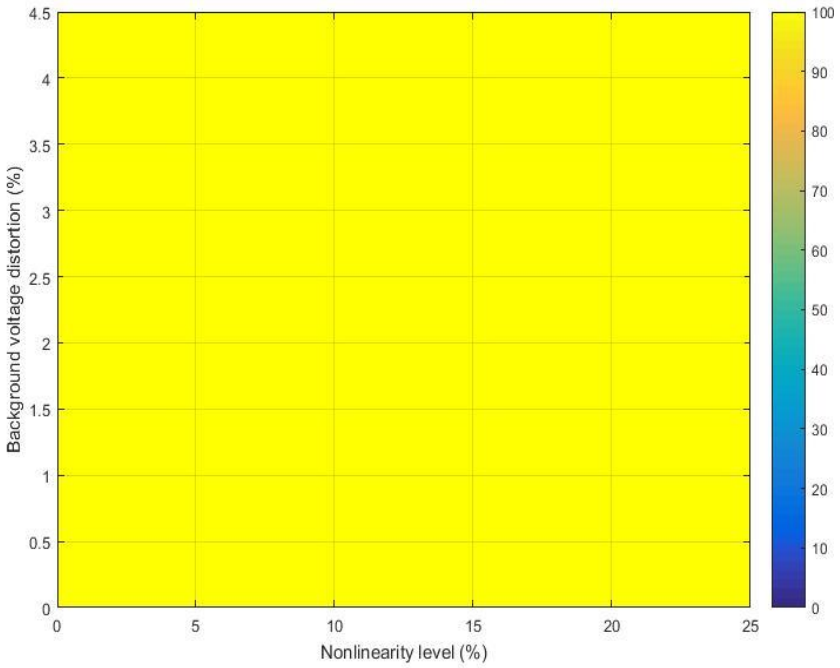

(a) Harmonic summation on the basis of the IEC summation rule

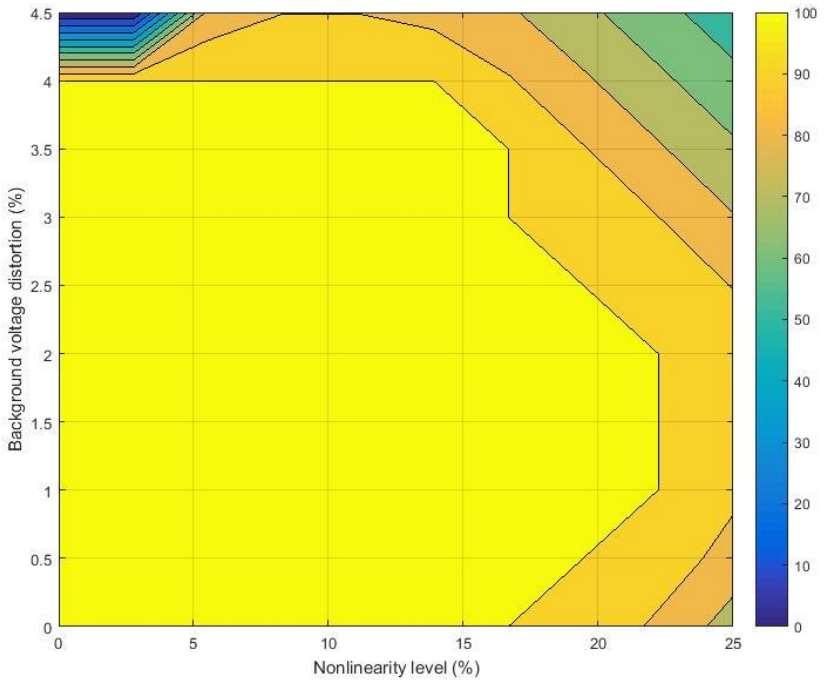

(b) Harmonic phasor summation

Fig. 8. Trends of the HC after applying the proposed filter

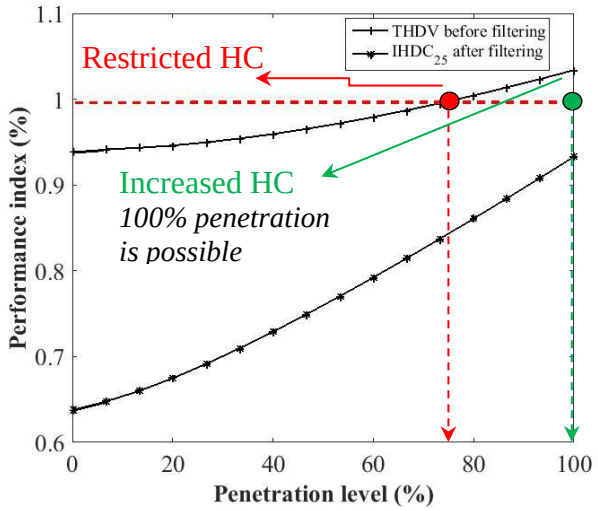

(a) 15% NLL and 4.5% BVD on the basis of the IEC summation rule

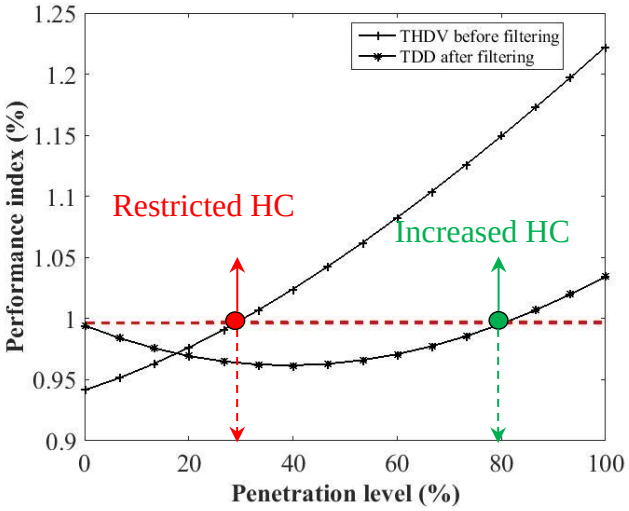

(b) 15% NLL and 4.5% BVD on the basis of the phasor summation

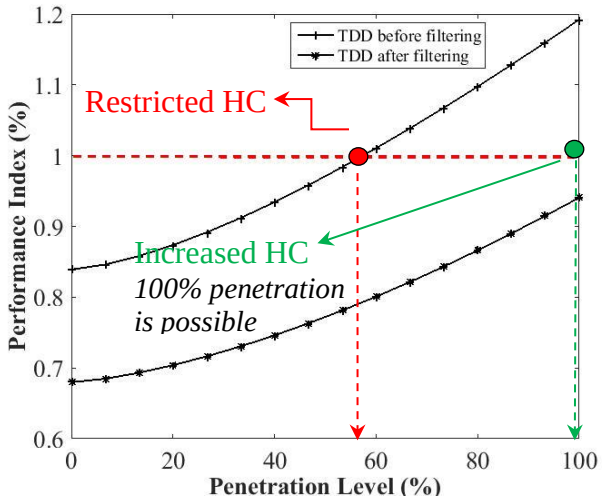

(c) 25% NLL and 0% BVD on the basis of the IEC summation rule

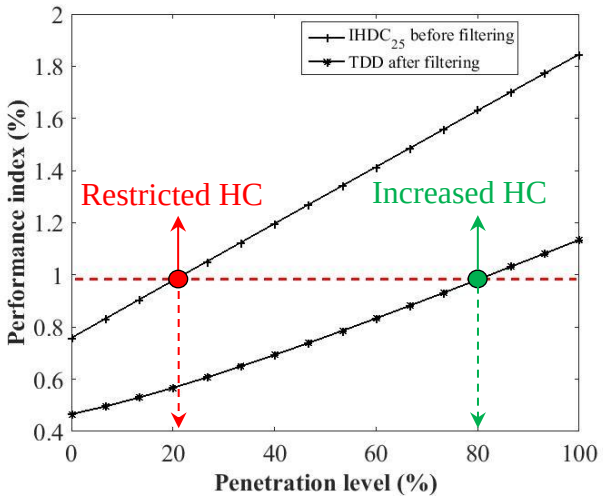

(d) 25% NLL and 0% BVD on the basis of the phasor summation

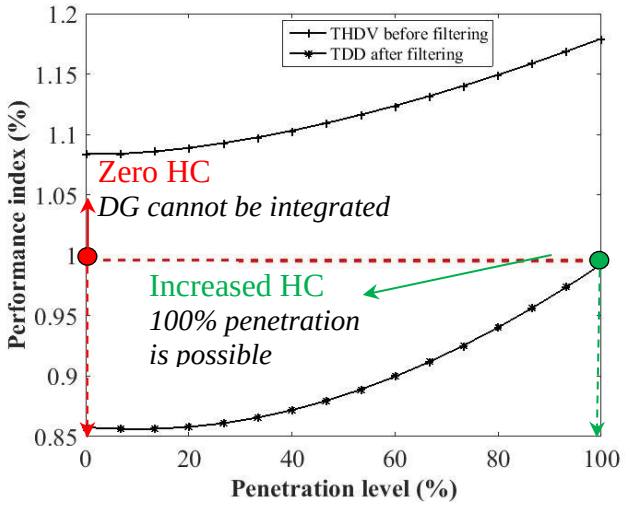

(e) 25% NLL and 4.5% BVD on the basis of the IEC summation rule

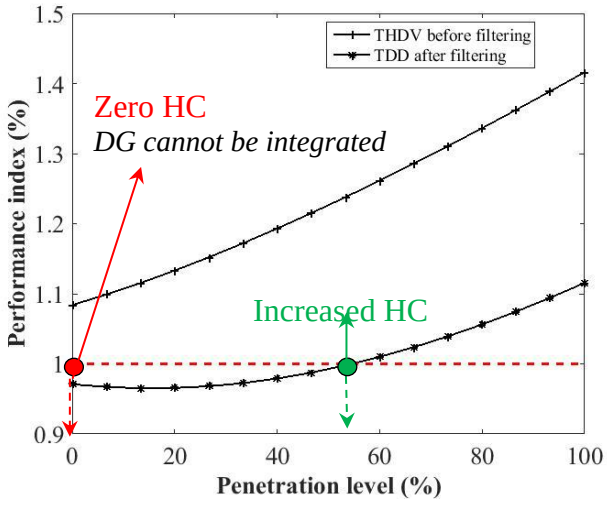

(f) 25% NLL and 4.5% BVD on the basis of the phasor summation

Fig. 9. HC assessment after applying the proposed filter at the considered levels

The obtained performance indices results of the designed filter via OF_1 at 25% NLL and 0% BVD in the frequency-domain analysis using the HPF are validated at the time-domain simulations by modelling of the system in the Simulink environment of MatLab software. Table 7 shows the reasonable agreement between both simulation results.

Table 7
Frequency-domain and time-domain simulation results of the proposed filter

Parameters	*THDV (%)*	*TDD (%)*	*PF (%)*	V_L *(p.u)*	ΔP_{loss} *(p.u.)*
Frequency-domain analysis	3.8415	1.7252	99.8776	0.9707	0.0245
Time-domain analysis	3.7200	1.7250	99.8829	0.9704	0.0256

4. CONCLUSIONS

In this paper, the HC determination of a distorted distribution system with Photovoltaic (PV)-based DG units is handled as an optimization problem by considering over and under voltage limitations of buses, current carrying capabilities of the lines, and harmonic distortion limitations as constraints. In the algorithm developed for the solution of the formulated optimization problem, the harmonic power flow method is used to calculate the harmonic components. Numerous simulations are conducted to show the effect of source and load nonlinearities on the studied system's hosting capacity. Results have demonstrated that the higher the harmonic distortion, the lower the hosting capacity of the system.

As a result, a *C*-type passive filter is designed to maximize the harmonic-constrained hosting capacity of the system, while enhancing the voltage, improving the power factor, and filtering the harmonics. The genetic algorithm has been used for the simultaneous determination of the optimal filter size and the maximum DG penetration level for the system. Here it should be noted that to show the validity of the results, the solution of the considered optimization problem is also found using Grid Search Method, which is one of the oldest and most reliable optimization methods.

The obtained results indicate that more hosting capacity can be achieved using the proposed filter design approach compared to three conventional filter design approaches, which are based on voltage total harmonic distortion minimization, line loss minimization and power factor maximization. Also, in the case of very high harmonic distortion levels and high power applications, active or hybrid combination of active and passive filters can be designed with the proposed objective function of maximizing the hosting capacity. A cost-benefit analysis should be undertaken in such cases because of the high active filters cost compared to the passive filters.

The results are limited to the peak instantaneous penetration and its direct impacts on the power quality of the system. Other factors that were beyond the framework of the study may be included in the optimization problem such as the economic constraints, and load alterations on yearly time-scales.

For a yearly time-scale, the proposed methodology can also be applied via using other types of inverters with enhanced capabilities. As the recent inverters have the ability to change the values of active power, reactive power, and the power factor in a wide range from 0.95 lagging to 0.95 leading automatically. This range of power factor is suitable to control the absorption and injection of the reactive power with load alterations. However, it should be mentioned that the inverters with these built-in facilities have considerably higher costs compared to the conventional inverters. In addition, other types of passive schemes such as switching filters or adaptive filters can be used to emphasize feeders with greater or lesser integration capacity under varying operating conditions. Investigations concerning these points will be presented in future works. In future works, the performances of the other metaheuristic optimization techniques are also comparatively evaluated for the sizing of the proposed filter design.

5. ACKNOWLEDGEMENT

Authours would like thank Prof. Dr. Mehmet Hakan Hocaoglu since his helpful and constructive comments to this paper.

This paper is supported by The Scientific and Technological Research Council of Turkey under the project 116E110.

6. REFERENCES

[1]. Jenkins N, Allan R, Crossley P, Kirschen D, Strbac G. Embedded Generation. IET Power and Energy Series 31, reprinted 2008.

[2]. Paliwal P, Patidar NP, Nema RK. Planning of grid integrated distributed generators: a review of technology, objectives and techniques. Renewable and Sustainable Energy Reviews. 2014; 40: 557-570.

[3]. Ackermann T, Anderson G, Söder L. Distributed generation: a definition. Electric Power Systems Research. 2001; 57: 195-204.

[4]. Mousa AGE, Abdel Aleem SHE, Ibrahim AM. Mathematical Analysis of Maximum Power Points and Currents Based Maximum Power Point Tracking in Solar Photovoltaic System: a Solar Powered Water Pump Application. Int Rev Electr Eng. 2016; 11:97-108

[5]. Bruni G, Cordiner S, Mulone V. Domestic Distributed Power Generation: Effect of Sizing and Energy Management Strategy on the Environmental Efficiency of a Photovoltaic- Battery- Fuel Cell System. Energy. 2014;77:133-143.

[6]. Li L, Mu H, Li N, Li M. Economical and Environmental Optimization for distributed Energy Resource System Coupled with District Energy Networks. Energy. 2016;109: 947-960.

[7]. Walling RA, Saint R, Dugan RC, Burke J, Kojovic LA. Summary of distributed resources impact on power delivery systems. IEEE Trans. on Power Delivery. 2008; 23; 1634-1644.

[8]. Guan FH, Zhao DM, Zhang X, Shan BT, Liu Z. Research on distributed generation technologies and its impacts on power system. *Int. Conf. on Sustainable Power Generation and Supply*. 2009;1-6.

[9]. Viral R, Khatod DK. Optimal planning of distributed generation systems in distribution system: a review. Renewable and Sustainable Energy Reviews, 2012;6:5146-5160.
[10]. Prakash P, Khatod K. Optimal sizing and siting techniques for distributed generation in distribution systems: a review. Renewable and Sustainable Energy Reviews. 2016; 57;111-130.
[11]. Esmaelli M, Sedighizadeh M, Esmaili M. Multi- Objective Optimal Reconfiguration and DG (Distributed Generation) Power Allocation in Distributed Networks Using big Bang-Big Crunch Algortihm Considering Load Uncertainty. Energy. 2016; 103: 86-99.
[12]. Davidson EM, Dolan MJ, Ault GW, McArthur SDJ. AuRA-NMS: An autonomous regional active network management system for EDF energy and SP energy networks. IEEE PES General Meeting; 2010 July 25-29, Minneapolis, MN: IEEE; 2010; 1-6.
[13]. Sultana U, Khairuddin A, Mokhtar AS, Zareen N, Sultana B. Grey wolf Optimizer Based Placement and Sizing of Multiple Disreibuted Generation in the Distribution System. Energy. 2016; 111: 525-536.
[14]. Prakash P, Khatod D. Optimal Sizing and Siting Techniques for Distributed Generation in Distirbution Systems: A Review. Renewable and Sustainable Energy Reviews. 2016;57: 111-130.
[15]. W Wanger VE. Effects of harmonics on equipment. IEEE Trans. on Power Delivery. 1993;8:672-680.
[16]. Balci ME, Emanuel AE. Apparent power definitions: a comparison study. Int. Review Elec. Engineering. 2011;6:2713-2722.
[17]. Balci ME, Hocaoglu MH. Effects of source voltage harmonics on power factor compensation in ac chopper circuits. Electrical Power Quality and Utilisation Journal. 2008;14: 53-60.
[18]. IEEE Recommended Practices and Requirements for Harmonic Control in Electrical Power Systems, IEEE 519, 2014.
[19]. Howmik AB, Maitra A, Halpin SM, Schatz JE. Determination of allowable penetration levels of distributed generation resources based on harmonic limit considerations. IEEE Trans. on Power Delivery. 2003;18:619-624.
[20]. Pandi VR, Zeineldin HH, Xiao W. Allowable DG penetration level considering harmonic distortions. 37th Annual Conf. on IEEE Industrial Electronics Society. 2011;814-818.
[21]. Dartawan K, Austria R, Hui L, Suehiro M. Harmonic issues that limit solar photovoltaic generation on distribution circuits. *Solar* 2012. 2012; 13- 17.
[22]. Sun W, Harrison GP, Djokic SZ. Distribution network capacity assessment: incorporating harmonic distortion limits. 2012 IEEE Power and Energy Society General Meeting. 2012;1-7.
[23]. Pandi VR, Zeineldin HH, Xiao W, Zobaa AF. Optimal penetration levels for inverter- based distributed generation considering harmonic limits. Electric Power Systems Research. 2013;97:68-75.
[24]. Santos N, Cuk V, Almeida PM, Bollen MHJ, Ribeiro PF. Considerations on hosting capacity for harmonic distortions on transmission and distribution systems. Electric Power Systems Research. 2015;119:199-206.
[25]. Mohammadi M, Rozbahani A, Montazeri M. Multi criteria simultaneous planning of passive filters and distributed generation simultaneously in distribution system considering nonlinear loads with adaptive bacterial foraging optimization approach. Int. Journal of Electrical Power & Energy Systems. 2016:79:253-262.
[26]. Ghaffarzadeh N, Sadeghi H. A new efficient BBO based method for simultaneous placement of inverter-based DG units and capacitors considering harmonic limits. Int. Journal of Electrical Power & Energy Systems. 2016;80: 37-45.

[27]. Xiao Y, Zhao Y, and Mao S. Theory for the Design of C-type Filter. 11th Int. Conf. Harmonics and Quality of Power, ICHQP. 2004.
[28]. Aleem SHE, Zobaa AF, Aziz MM. Optimal C-type passive filter based on minimization of the voltage harmonic distortion for nonlinear loads. IEEE Trans. on Industrial Electronics. 2012;59: 281-289
[29]. Abdel Aleem SHE, Balci ME, Sakar S, Optimal passive filter design for effective utilization of cables and transformers under non-sinusoidal condition. Journal of Electric Energy and Power Systems. 2015;71:344-350.
[30]. High Penetrations of Renewable Energy For Island Grids Reports, http://www.power-eng.com/content/pe/en/articles/print/volume-111/issue-11/features/high-penetrations-of-renewable-energy-for-island-grids.html.
[31]. Sun W. Maximizing Renewable Hosting Capacity in Electricity Networks. Doctor of Philosophy. 2015. The University of Edinburg.
[32]. Thesis: https://uu.diva-portal.org/smash/get/diva2:833570/FULLTEXT01.pdf.
[33]. I IEC 61000-3-6, Electromagnetic Compatibility (EMC)-Part 3-6: Limits- Assessment of Emission Limits for the Connection of Distorting Installations to MV, HV and EHV Power System, 2008.
[34]. Chico G, Schlaabbach J, Spertino F. Operation of Multiple Inverters in Grid- Connected Large-Size Photovoltaic Installations. 20th International Conference on Electricity Distribution. 2009.
[35]. ANSI C84.1. NEMA Standard. 2011.
[36]. IEEE P1547, 'Standard for Distributed Resources Interconnected With Electric Power Systems', Sep. 2002.
[37]. Aleem SHE, Ibrahim AM, Zobaa AF. Harmonic Assessment Based Adjusted Current Total Harmonic Distortion. The Journal of Engineering. 2016. DOI: 10.1049/joe.2016.0002
[38]. Mathworks Documentation. http://www.mathworks.com/help/gads/ga.html?searchHighlight=ga, 2015.
[39]. David E. A Detailed Analysis of sis- Pulse Converter Harmonic Currents. IEEE Trans. On Industrial. Applications. 1994;30:294-304.
[40]. Olive AR, Balda JC. A PV dispersed generator: a power quality analysis within the IEEE 519. IEEE Trans. On Power Delivery. 2003;18:525- 530